Electronic Supplementary Material (ESI) for New Journal of Chemistry.
This journal is © The Royal Society of Chemistry and the Centre National de la Recherche Scientifique 2024

Sunlight Irradiated efficient Photocatalytic Oxidation of Benzylamines and CO_2 Reduction over 2D-2D MoS_2/FP-BTA Heterojunction Catalyst

Surya Das,[a] Priyanka Sarkar,[a] Anil Chandra Kothari, [b,c] Manoj Goswami, [d] Aslam Khan, [e] and Sk. Manirul Islam, [a]*

[a] *Department of Chemistry, University of Kalyani, Kalyani, Nadia, 741235, W.B., India.*

[b] *Light Stock Processing Division, CSIR-Indian Institute of Petroleum, Dehradun 248005, Uttarakhand, India*

[c] *Academy of Scientific and Innovative Research (AcSIR), Ghaziabad, 201002, India*

[d] *CSIR-Advanced Materials and Processes Research Institute (AMPRI), Bhopal 462026, India*

[e] *King Abdullah Institute for Nanotechnology, King Saud University, Riyadh, 11451, Saudi Arabia*

*Email: manir65@rediffmail.com

---

1. Materials

Phloroglucinol and hexamethylenetetramine (HMTA) were received from sigma Aldrich, India. Hydrazine, trifluoroacetic acid, 4-nitroaniline, and 1,3,5- benzene-tri-carbonyl-trichloride were purchase from TCI, India. 1,4 dioxane, acetone, tetrahydrofuran (THF), N, N-dimethylformamide (DMF), and acetonitrile were obtained from Merck, India and used without further purification. Benzylamine derivatives were bought from sigma Aldrich, TCI Chemicals (India) and BLD pharm. All other reagents and solvents were bought from E-Merk, India and were used as received. The CO_2 and O_2 gas cylinder were acquired from Apollo Engineering Gas Service, India. All the reactions were performed using oven-dried Schlenk balloon set-up technique.

2. Instrumentation

Absorption spectroscopy: UV-vis absorption spectra of the catalyst was recorded on SHIMADZU, UV-2600 UV-vis spectrometer with a standard 1 cm x 1 cm cuvette.

NMR Spectra: ^{1}H NMR (Proton nuclear magnetic resonance spectra) were performed on a Bruker 400 MHz spectrometer. Chemical shifts for protons are reported in parts per million (ppm).

PXRD: The PXRD analysis of the photocatalyst (MoS_2/FP-BTA) was executed by using an X-ray diffractometer (BRUKER, Powder X-Ray ecoD8 ADVANCE) equipped with Ni-filtered Cu Kα (λ= 0.15406 nm) radiation.

IR Spectra: The FTIR spectra of the synthesized and starting materials were conducted by using a Perkin-Elmer spectrophotometer (FT-IR 783) on KBr Pellets.

FESEM: FESEM images of the catalyst were acquired by using Scanning Electron Microscope (SEM) [JEOL JSM IT 300], which help to know about the morphological information of the sample.

TEM: Transmission Electron Microscope (TEM) [JEOL JEM 2100] was used to get the morphological information of the sample.

TGA: The thermal stability of the MoS_2/FP-BTA material was analysed by a Thermogravimetric Analyzer [Model: Perkin Elmer-Pyrish-Diamond, TG/DTA] at the rate of 10 °C per min up to 800 °C in presence of air.

BET: The N2 adsorption-desorption analysis of MoS_2/FP-BTA sample was conducted by using a BET Surface Analyzer [QUANTACHROME ASIQCOV602-5].

Fluorescence Spectroscopy: The Fluorescence Emission spectra was recorded by using Horiba Fluoro Max 4 spectrometer.

EIS analysis: The measurements have been performed in 0.1 M PBS solution and a conventional three-electrode system where MoS_2/FP-BTA catalyst on the glassy carbon

electrode is used as the working electrode and double junction Ag/AgCl saturated with 3.0M KCl is used as a reference electrode. The Platinum wire served as a counter electrode. The electrochemical impedance spectroscopy (EIS) has been carried out in the frequency range of 100 kHz -0.01 Hz with an AC amplitude of 10 mV at a constant the applied potential of 5 mV.

Preparation of the catalyst

Schematic presentation for the synthesis of the MoS_2 loaded covalent organic framework-heterojunction catalyst (MoS_2/FP-BTA) is shown in Scheme 2 in the manuscript.

General procedure for the production of 2,4,6-Triformylphluroglucinol (FP)

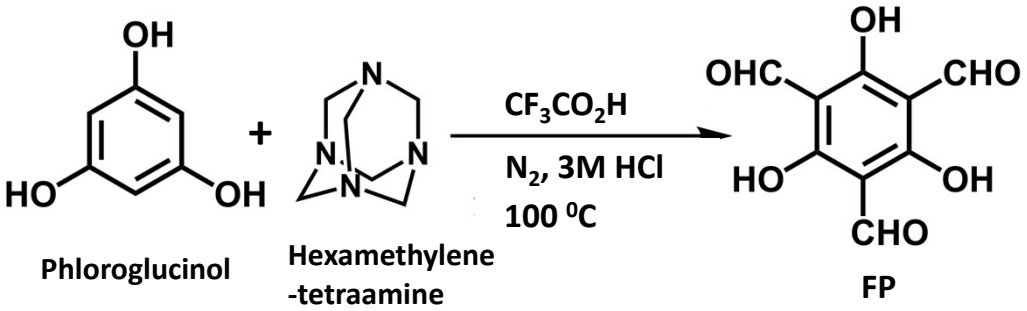

Figure S1: Preparation of 2,4,6-Triformylphluroglucinol (FP).

Synthesis of 2,4,6-Triformylphluroglucinol (FP) was prepared according to the preceding literature.[1] In a brief, trifluoroacetic acid (90 mL), hexamethylene tetramine (108 mmol) and dried phloroglucinol (49 mmol) were placed in a 500 ml round bottom flask and the flask was heated at 100 ^{0}C for 2.5 hours under N_2 environment. 3M hydrochloric acid (150 ml) was added very carefully to the resulting solution, which was then constantly stirred for a further hour at a predetermined temperature. After cooling to room temperature, the solution was extracted with dichloromethane (DCM) and dried over anhydrous sodium sulphate (Na_2SO_4). The acquired extract was concentrated to produce a dull yellow colour solid and the crude

solid was then further purified by hot ethanol to produce desired product (FP). ^{1}H NMR (298K, 400 MHz, DMSO-d6) δ/ppm: 14.05 (s, 1H), 10.09 (s, 1H).

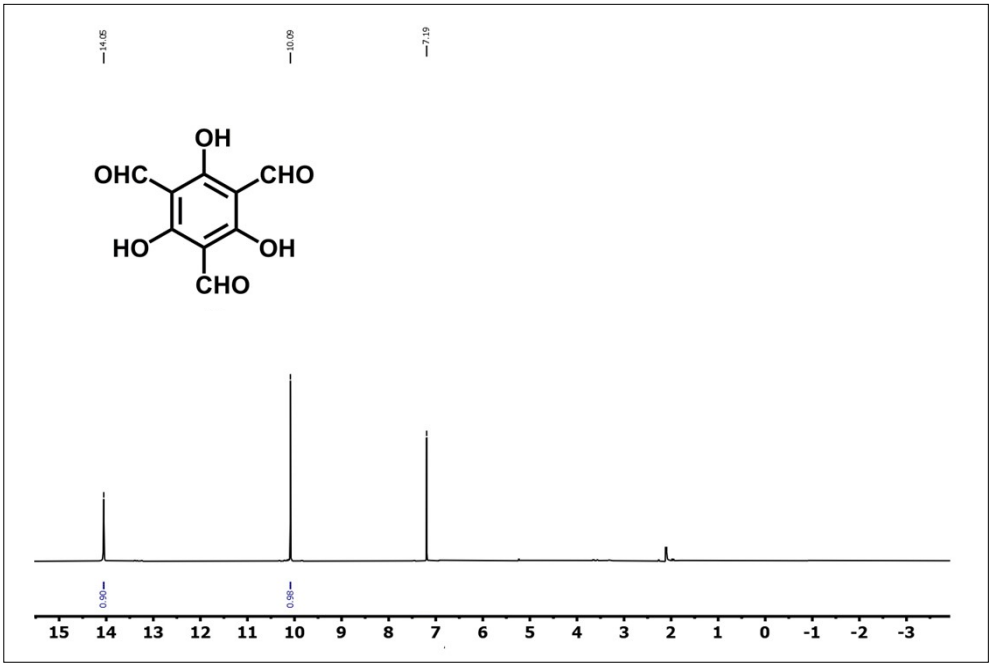

Figure S2.^{1}H NMR spectra of 2,4,6-triformylphloroglucinol (FP).

General procedure for the production of *N*^{1}, *N*^{3}, and *N*^{5}-tris-(4-aminophenyl) benzene-1, 3, 5-tricarboxamide (BTA)

BTA was synthesized according to previous reported literature [2]. Firstly, 4-nitroaniline (2g) was dissolved in acetonitrile solvent (30 ml) and 1, 3, 5- benzene- tricarbonyl- trichloride (0.465 g) was then added to it. The reaction mixture was continuously stirred for overnight under reflux condition at 85 ^{0}C. The resulting material was allowed to filtered and washed multiple times with cold acetonitrile (CH_3CN) solvent. The obtained nitro derivative was suspended in 23 mL dimethyl dimethylformamide (DMF). Then ethyl alcohol (23 ml) and 10% Pd/C (13 mg) was added to the above solution mixture. After that hydrazine monohydrate (2.65 g, 52.9 mmol) was added drop wise and the whole reaction mixture was continuously stirred

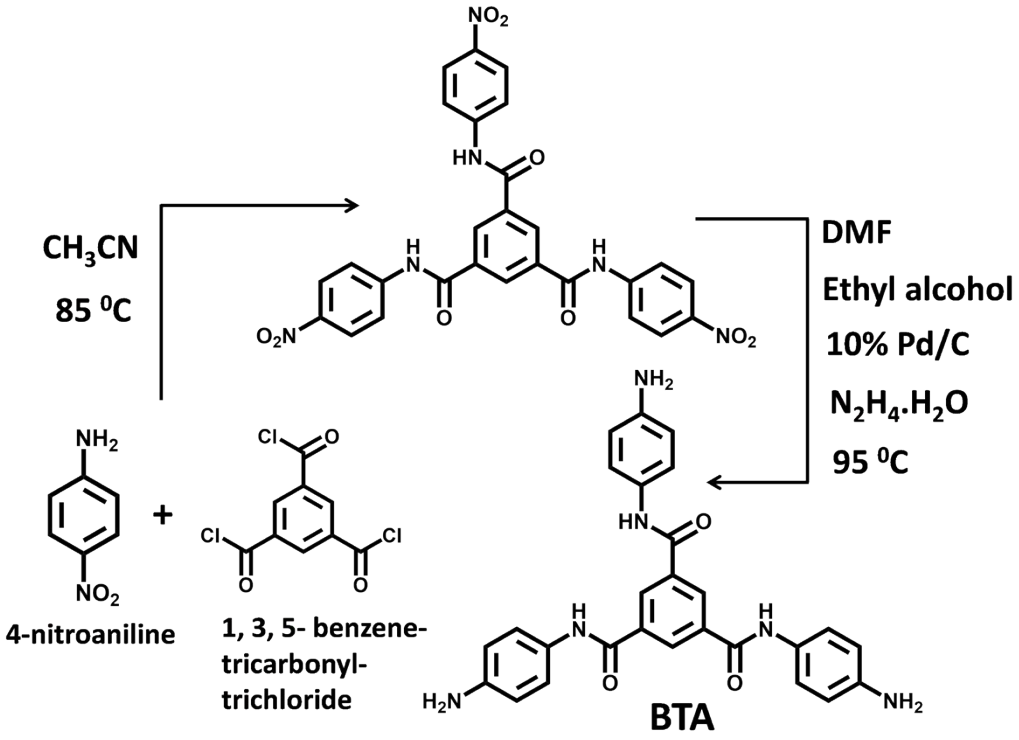

Figure S3: Preparation of N^1, N^3, and N^5-tris-(4-aminophenyl) benzene-1, 3, 5-tricarboxamide (BTA).

for 24 hours at 95 ^{0}C under nitrogen environment. After the completion of the reaction, the hot mixture was filtered and washed with hot ethanol. The yellow-coloured filtrate was collected and excess amount of water was added to the solution. The resulting precipitate was isolated by centrifugation and dried under vacuum to obtain BTA as a yellow solid (79% yield). ^{1}H NMR (298K, 400 MHz, DMSO-d6) δ/ppm: 10.175 (s, 3H), 8.563 (s, 3H), 7.415 (d, J = 8.4, 6H), 6.56 (d, J = 8.4, 6H), 4.997 (s, 6H).

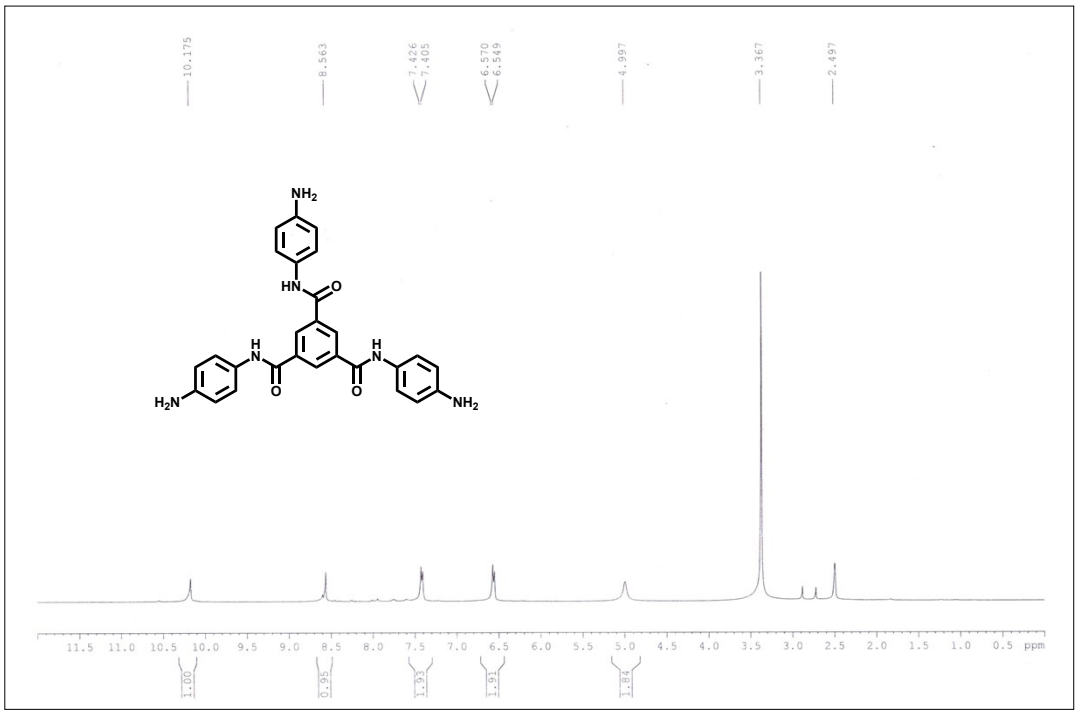

Figure S4. ^{1}H NMR spectra of N^{1}, N^{3}, and N^{5}-tris-(4-aminophenyl) benzene-1, 3, 5-tricarboxamide (BTA)

Synthetic Procedure of FP-BTA COF

The construction path of porous FP-BTA covalent organic framework (FP-BTA COF) were depicted in Scheme 2 in the manuscript. As per previously published literature, 2,4,6-triformylphluroglucinol (FP) was produced using phloroglucinol, hexamethylenetetramine, and trifluoroacetic acid [1]. N^{1}, N^{3}, and N^{5}-tris-(4-aminophenyl) benzene-1, 3, 5-tricarboxamide (BTA) was also generated utilising the method that was previously described [2]. The β-keto-enamine linked FP-BTA COF was generally synthesized by thoroughly adding the 2, 4, 6-triformylphluroglucinol (FP, 0.18 mmol, 37.8 mg) and N^{1}, N^{3}, and N^{5}-tris-(4-aminophenyl) benzene-1, 3, 5-tricarboxamide (BTA, 0.18 mmol, 86.5 mg) monomer units, in a 5.5 mL solution of tetrahydrofuran (THF), mesitylene and 6M acetic acid (a specific ratio, v:v:v = 5:5:1) in 25 ml round bottom flask while stirring continuously. After being homogeneous by ultrasonic treatment for 15 minutes, the solution mixture was degassed to get rid of the air. The round bottom flask was then appropriately sealed off and heated at 120

^{0}C for three days in a row to accomplish the solvothermal procedure. Upon cooling to room temperature, the resultant precipitate was centrifuged to separate and then washed it in tetrahydrofuran (THF) and acetone one-by-one to eliminate unreacted reactants and existing contaminants from the obtained material to get pure orange coloured FP-BTA COF. Ultimately, the pure product was collected and dried in vacuum for 24 h to acquire FP-BTA COF as an orange powder with 81% yield. The powder FP-BTA COF was completely insoluble in water (H_2O) and a broad range of organic solvents, including tetrahydrofuran (THF), ethanol, acetone, N, N-dimethylformamide (DMF), hexanes, and others.

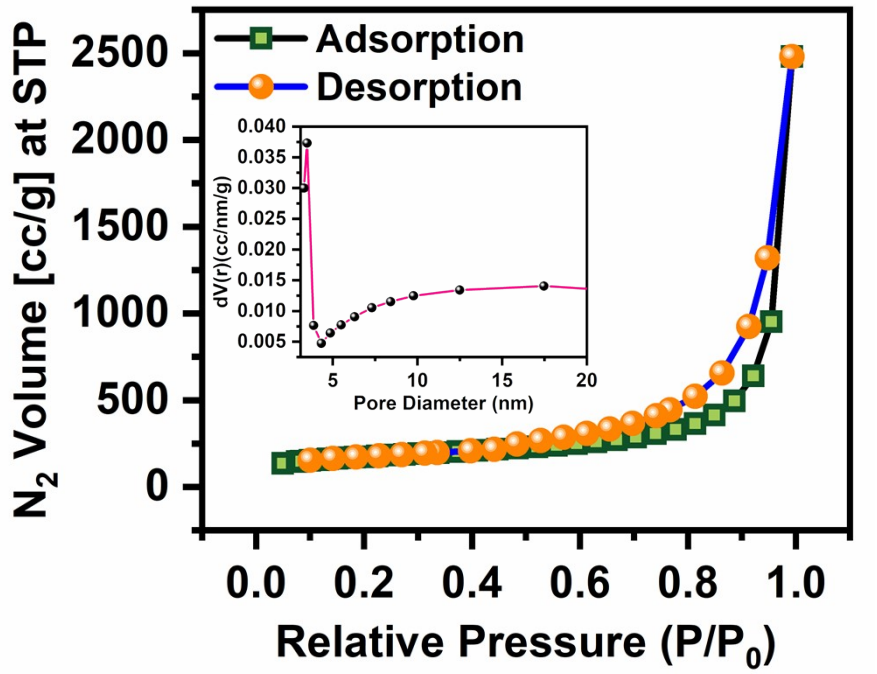

Figure S5. BET isotherm analysis and pore size distribution (PSD) curve (inset) of FP-BTA. COF.

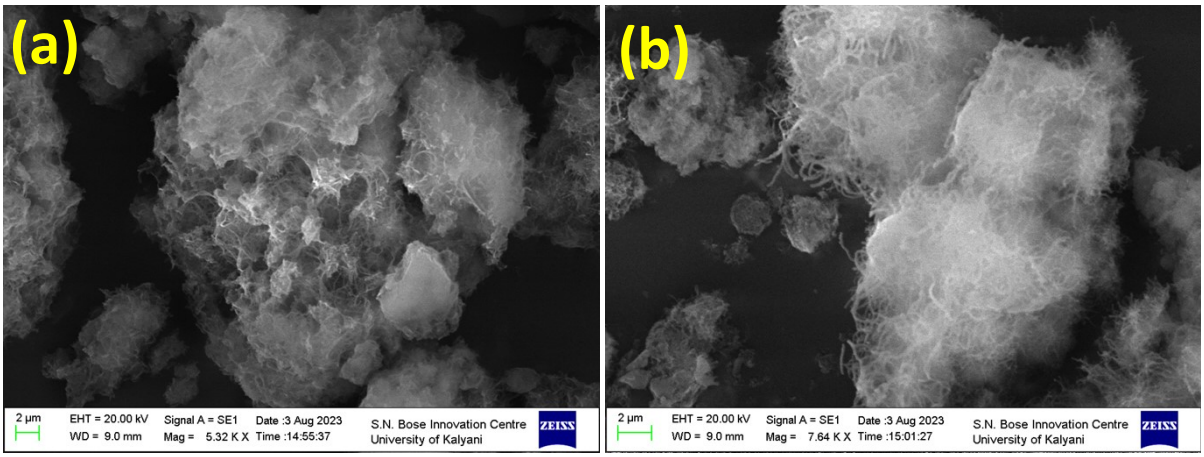

Figure S6. FE-SEM images of FP-BTA COF.

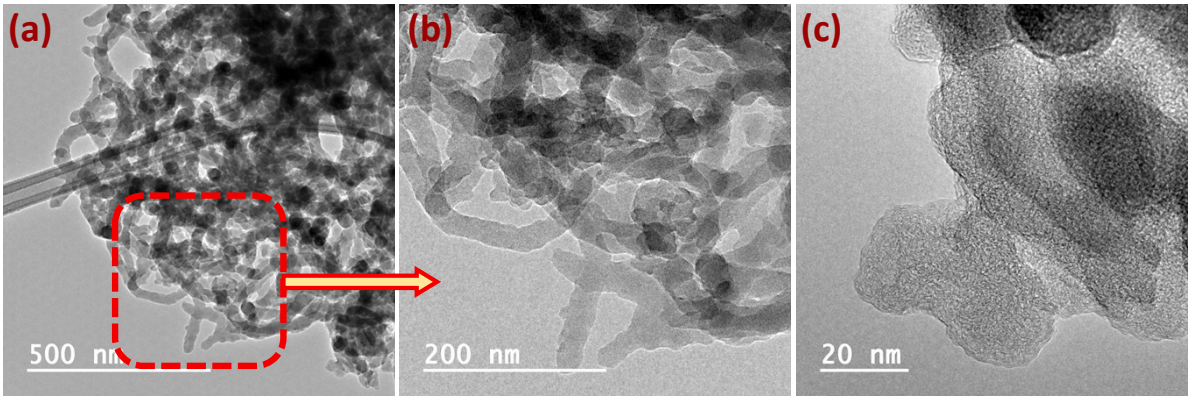

Figure S7. The HR-TEM pictures of FP-BTA COF at various magnifications (a) 500 nm, (b) 200 nm, and (c) 20 nm.

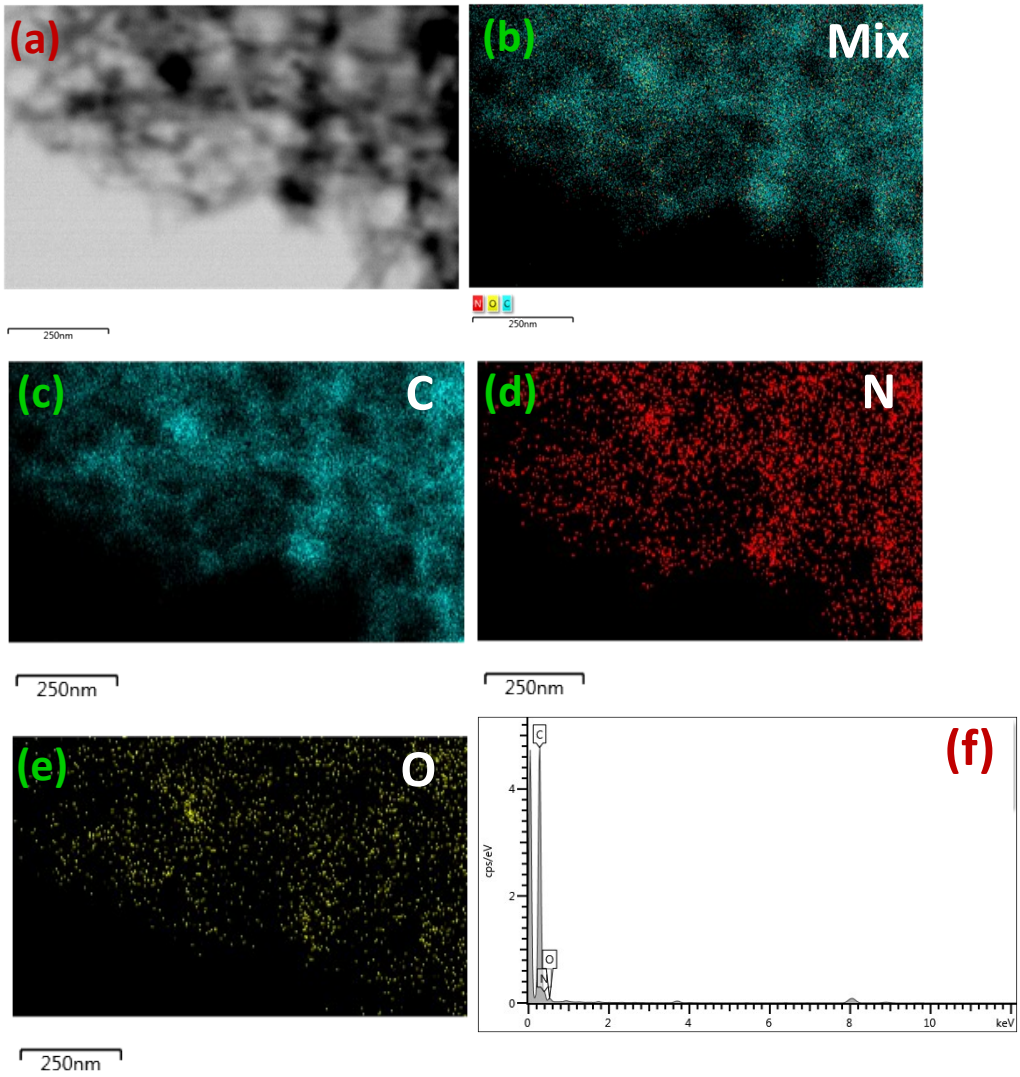

Figure S8. (a) Electron image of FP-BTA COF; Elemental mapping images of (b) FP-BTA COF: EDS mapping of (c) C, (d) N, (e) O elements, (f) EDX of FP-BTA COF.

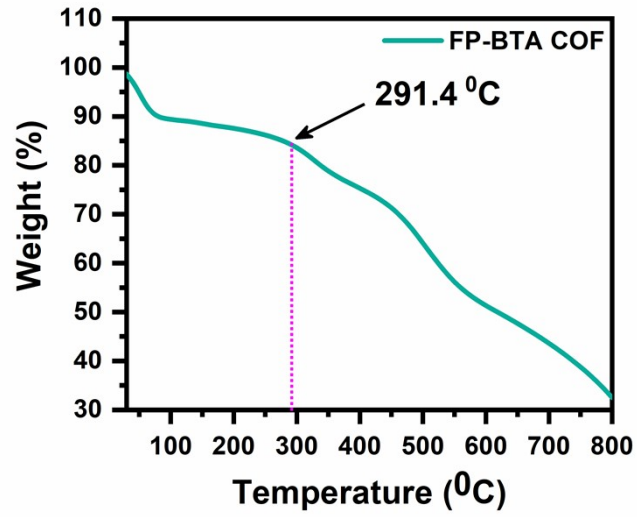

Figure S9. TGA plot of FP-BTA COF.

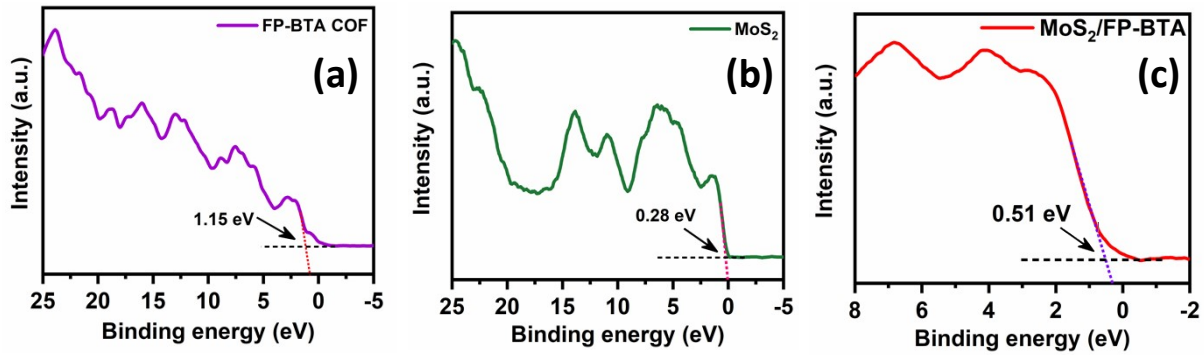

Figure S10. Valence-band (VB) XPS spectra of (a) FP-BTA COF, (b) MoS_2 and (c) MoS_2/FP-BTA heterojunction.

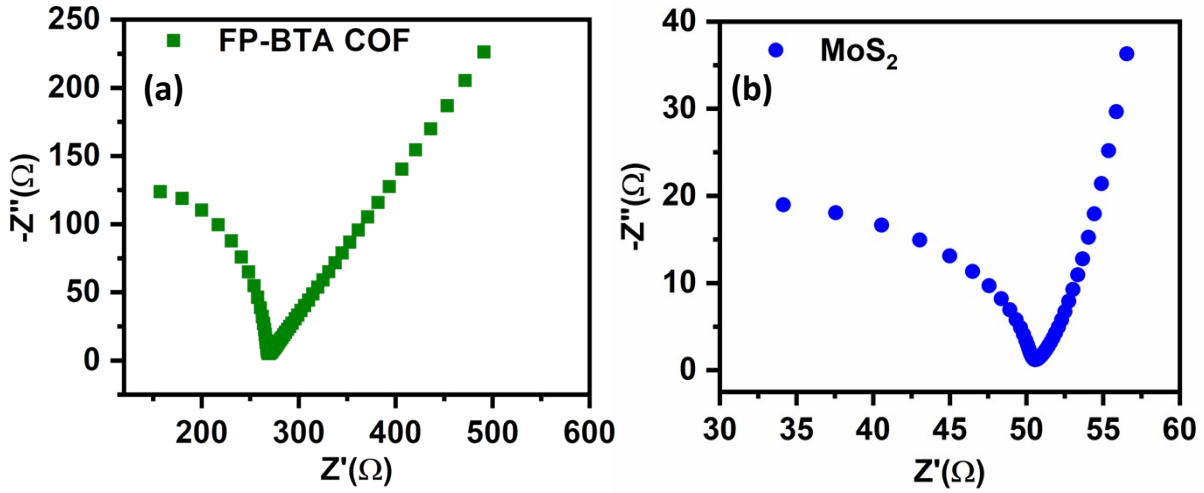

Figure S11. The electrochemical impedance spectroscopy (EIS) of (a) FP-BTA and (b) MoS_2.

Calculation of Yield of formic acid (HCOOH):

The yield of HCOOH was determined utilising a calibration plot, which is displayed in Figures S4, where the known concentrations of HCOOH were plotted with the O.D. values in UV-vis spectra to derive the concentrations of produced HCOOH.

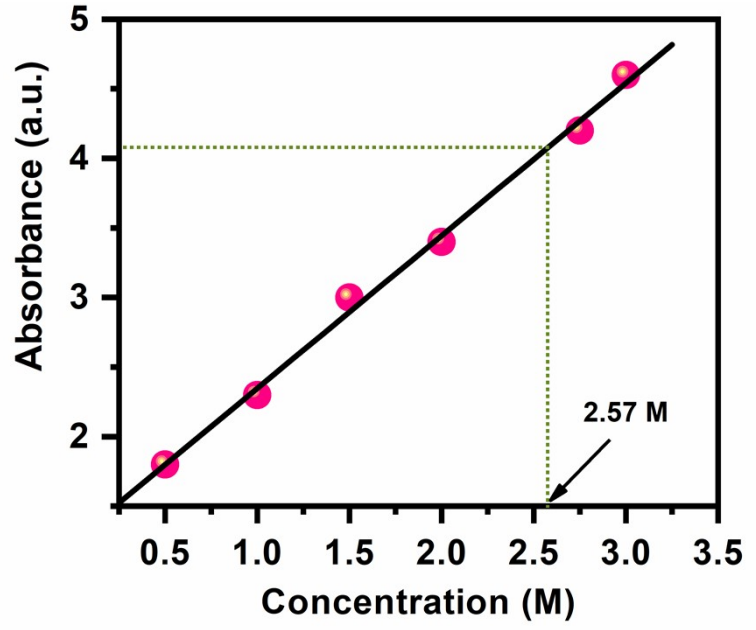

Figure S12. Calibration curve of HCOOH for determination of concentration of HCOOH produced.

Kinetic curve (yield vs. time) for the reaction:

We have examined the yield of the reactions with time in presence of the catalyst [MoS2/FP-BTA] and the kinetic curve has been plotted from the acquired data.

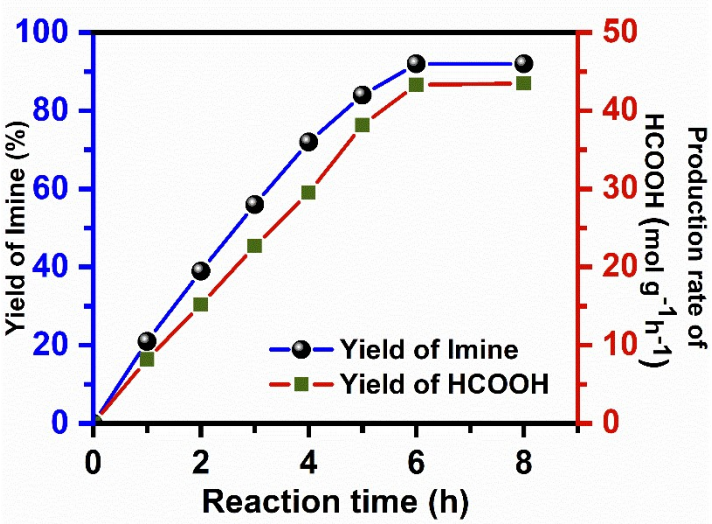

Figure S13. Kinetic curve for the production of Imine and HCOOH.

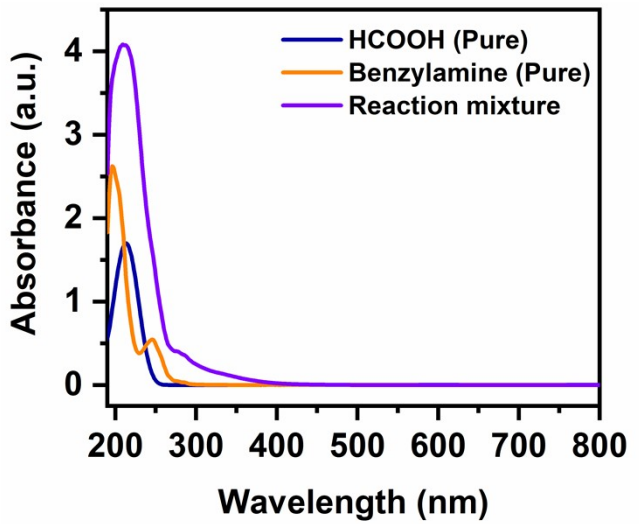

Figure S14: Adsorption Spectra of pure HCOOH, pure benzylamine and reaction mixture containing HCOOH after photocatalytic CO_2 reduction in acetonitrile solvent.

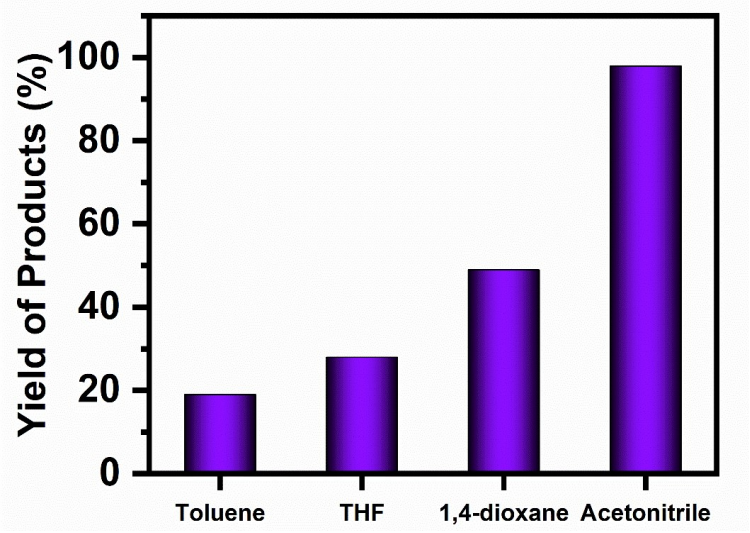

Figure S15. Yield of products in presence of O_2 under different solvents.

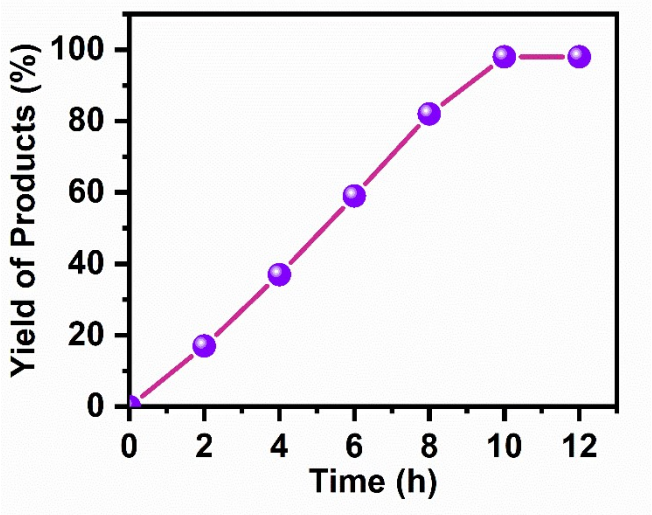

Figure S16. Kinetic curve for the production of products in presence of O_2.

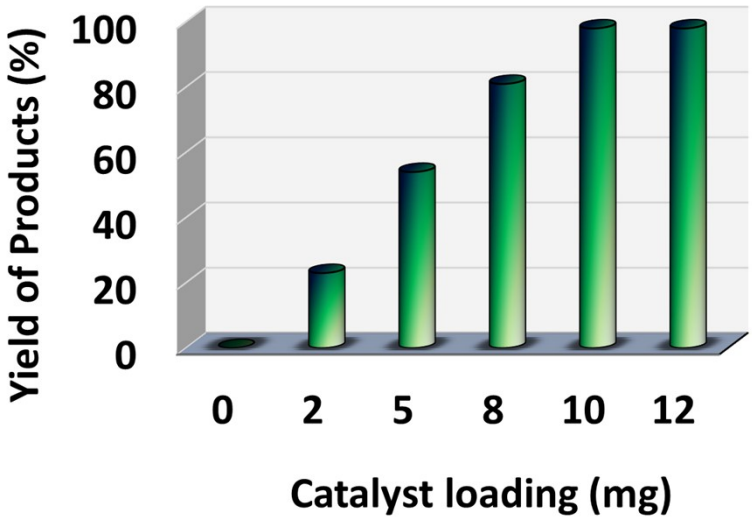

Figure S17. Variation of catalyst quantity for the production of products in presence of O_2.

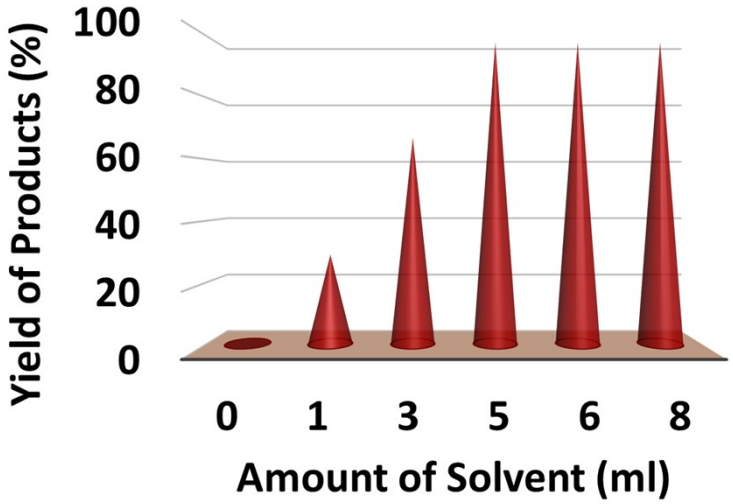

Figure S18. Variation of Acetonitrile solvent quantity for the production of products in presence of O_2.

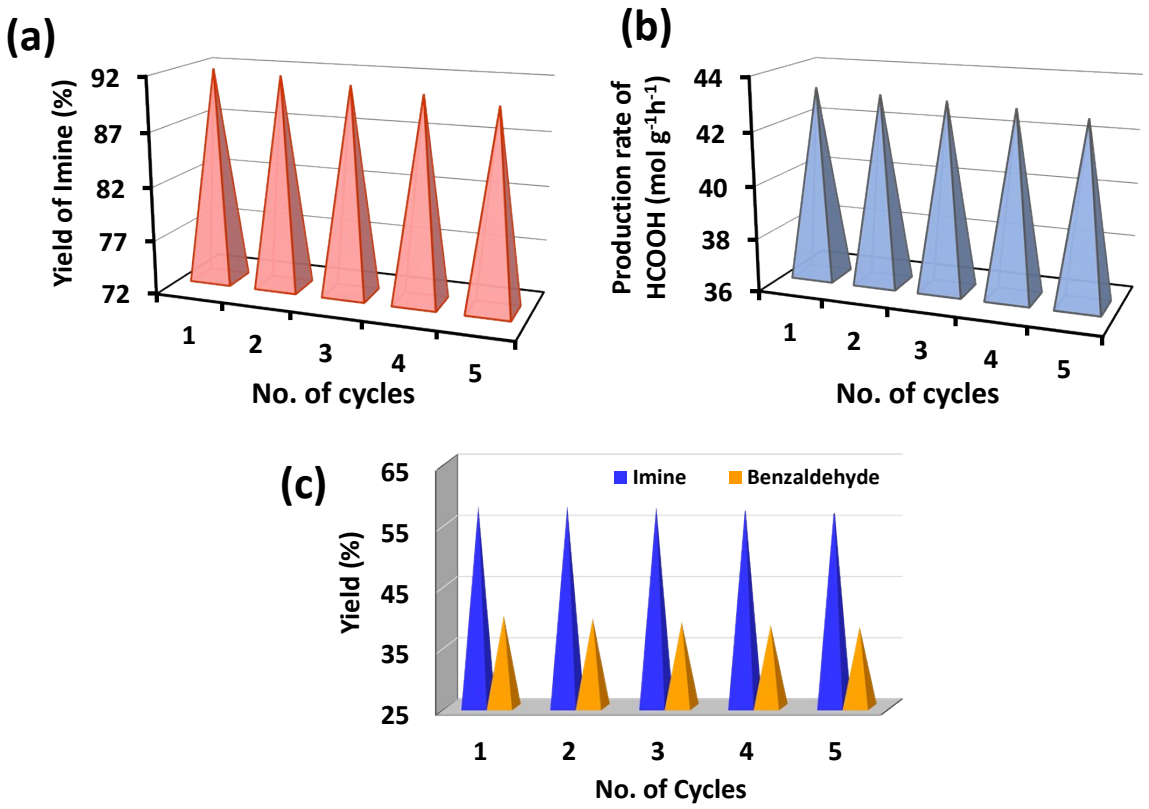

Figure S19. Recyclability of MoS_2/FP-BTA heterojunction.

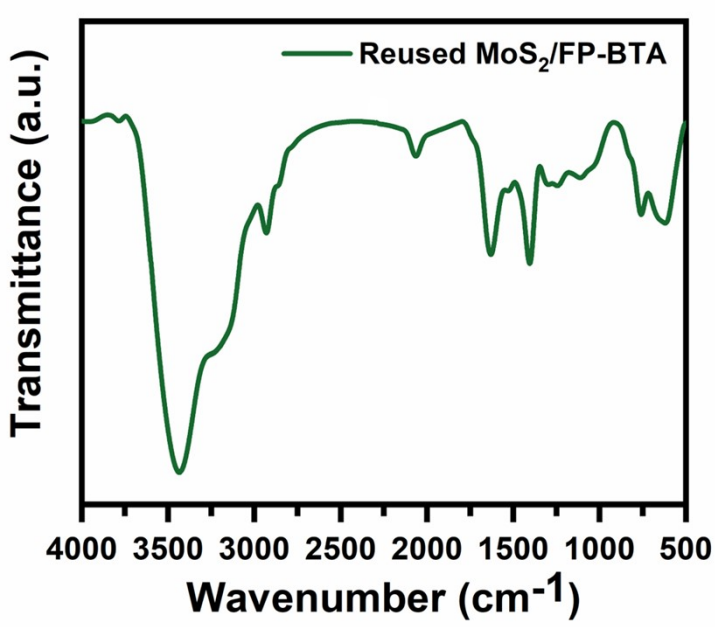

Figure S20. FT IR spectra of the reused MoS_2/FP-BTA heterojunction Catalyst

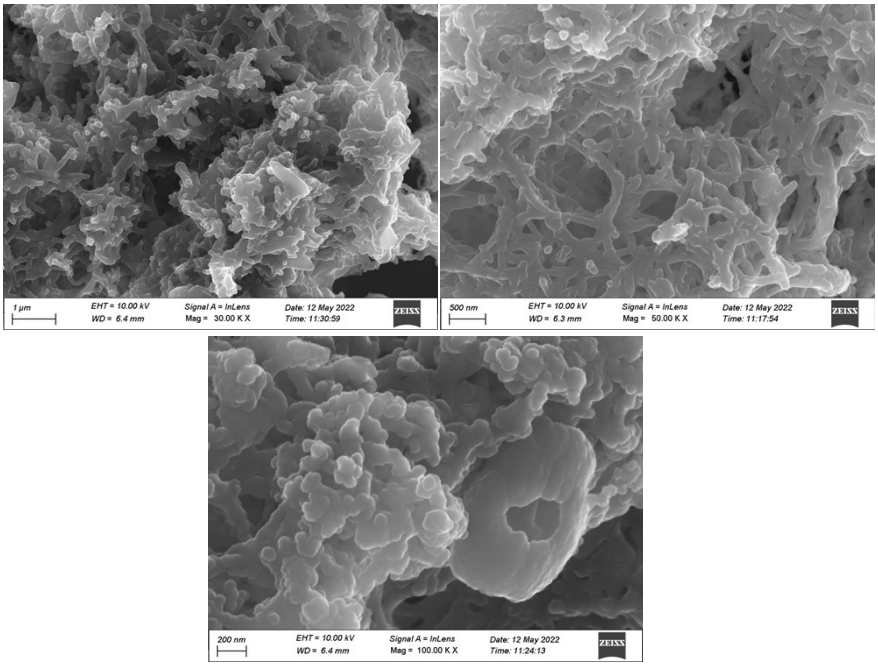

Figure S21. FE-SEM image of reused MoS_2/FP-BTA heterojunction catalyst

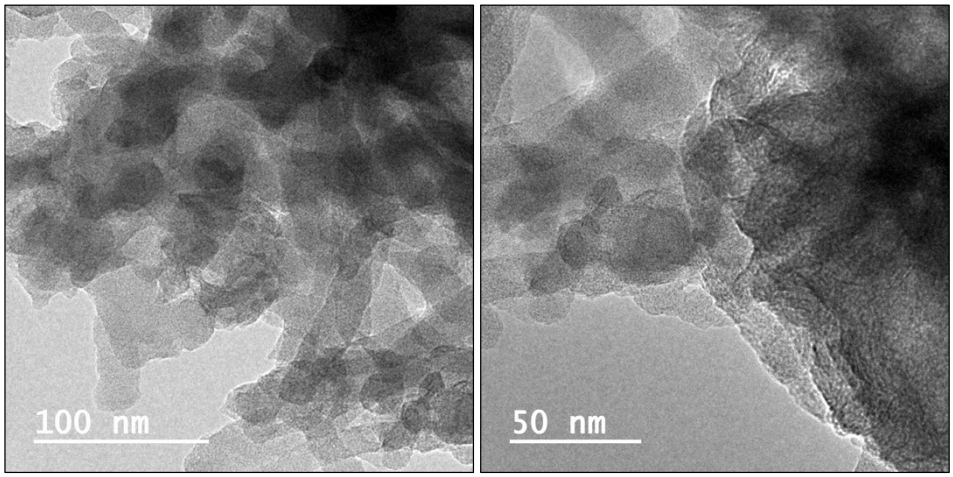

Figure S22. HR-TEM image of reused MoS_2/FP-BTA heterojunction catalyst.

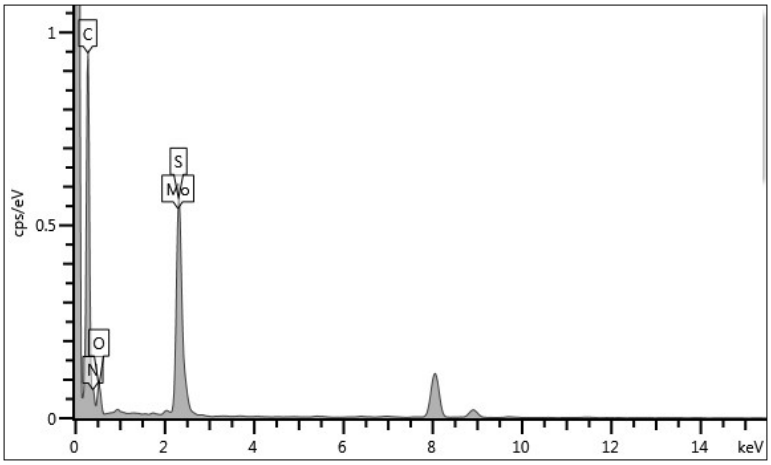

Figure S23. EDX of reused MoS_2/FP-BTA heterojunction catalyst.

^{1}H NMR data of N-benzylidene benzylamine amine derivatives in presence of CO_2:

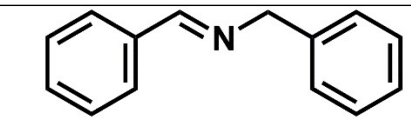	N-benzylidene benzylamine, ^{1}H NMR (400 MHz, $CDCl_3$), δ (ppm): 8.319 (s, 1H), 7.72-7.696 (m, 2H), 7.348-7.321 (m, 3H), 7.271-7.260 (d, *J*=4.4 Hz, 4H), 7.205-7.168 (m, 1H), 4.751 (s, 2H).
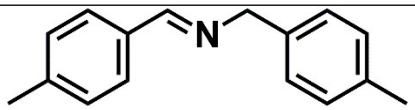	N-(4-methylbenzyl)1-(*p*-tolyl) methanimine, ^{1}H NMR (400 MHz, $CDCl_3$), δ (ppm): 8.253 (s, 1H), 7.591-7.571 (d, *J*=8.0 Hz, 2H), 7.146-7.119 (m, 4H), 7.073-7.053 (d, *J*=8.0 Hz, 2H), 4.682 (s, 2H), 2.294 (s, 3H), 2.251 (s, 3H).
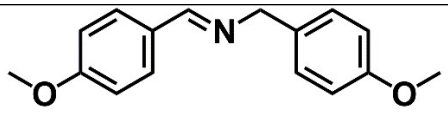	N-(4-methoxybenzyl)-1-(4-methoxyphenyl)methanimine, ^{1}H NMR (400 MHz, $CDCl_3$), δ (ppm): 8.217 (s, 1 H), 7.641–7.619 (d, 2 H), 7.174-7.153 (d, *J*=8.4 Hz, 2H), 6.849-6.827 (d, *J*=8.8 Hz, 2H), 6.807-6.786 (d, *J*=8.4 Hz, 2H), 4.641 (s, 2H), 3.749 (s, 3 H), 3.738 (s, 3 H).
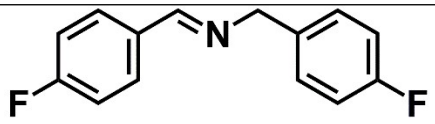	N-(4-fluorobenzyl)-1-(4-fluorophenyl)methanimine, ^{1}H NMR (400 MHz, $CDCl_3$), δ (ppm): 8.266 (s, 1 H), 7.708–7.672 (m, 2H), 7.231-7.178 (m, 2H), 7.043-6.929 (m, 4H), 4.684 (s, 2H).
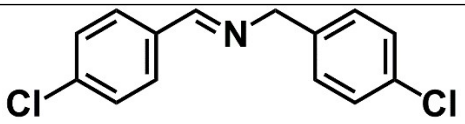	N-(4-chlorobenzyl)-1-(4-chlorophenyl)methanimine, ^{1}H NMR (400 MHz, $CDCl_3$) δ (ppm): 8.262 (s, 1H), 7.648-7.621 (m, 2H), 7.324-7.303 (m, 2H), 7.248-7.173 (m, 4H) 4.689 (s, 2H).

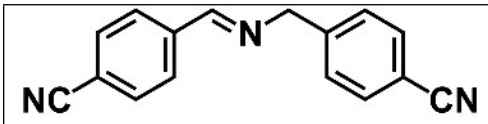	4-(((4-cyanobenzyl)imino)methyl)benzonitrile, ^{1}H NMR (400 MHz, $CDCl_3$) δ (ppm): 8.389 (s, 1H), 7.838-7.817 (d, *J*=8.4 Hz, 2H), 7.660-7.640 (d, *J*=8.0 Hz, 2H), 7.580-7.560 (d, *J*=8.0 Hz, 2H), 7.410-7.390 (d, *J*=8.0 Hz, 2H), 4.832 (s, 2H).
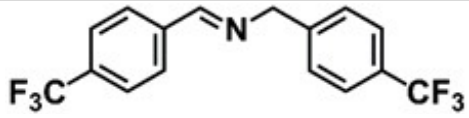	N-(4-(trifluoromethyl) benzyl)-1-(4-fluoromethyl) phenyl) methanimine, ^{1}H NMR (400 MHz, $CDCl_3$) δ (ppm): 8.489 (s, 1H), 7.944-7.918 (d, *J*=8.4 Hz, 2H), 7.725-7.699 (d, *J*=10.4 Hz, 2H), 7.652-7.624 (d, *J*=11.2 Hz, 2H), 7.507-7.480 (d, *J*=10.8 Hz, 2H), 4.923 (s, 2H).
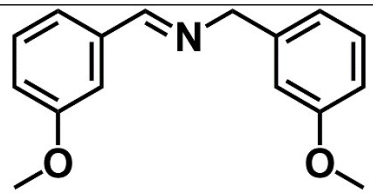	N-(3-methoxybenzyl)-1-(3-methoxyphenyl)methanimine, ^{1}H NMR (400 MHz, $CDCl_3$) δ (ppm): 8.233 (s, 1H), 7.291 (s, 1H), 7.231-7.133 (m, 3H), 6.888-6.806 (m, 3H), 6.716-6.690 (dd, *J*=8.4, 2.4 Hz, 1H), 4.683 (s, 2H), 3.735 (s, 3H), 3.665 (s, 3H).
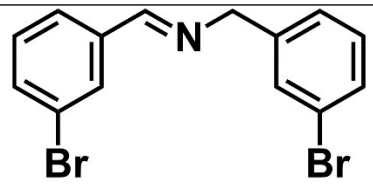	N-(3-bromobenzyl)-1-(3-bromophenyl)methanimine, ^{1}H NMR (400 MHz, $CDCl_3$) δ (ppm): 8.239 (s, 1H), 7.889 (s, 1H), 7.600-7.470 (m, 2H), 7.335-7.119 (m, 5H), 4.698 (s, 2H).
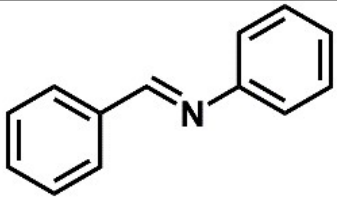	N,1-diphenylmethanimine, ^{1}H NMR (400 MHz, $CDCl_3$) δ (ppm): 8.386 (s, 1H), 7.022-7.785 (m, 10H).

Figure S24. [1]H NMR data of N-benzylidene benzylamine.

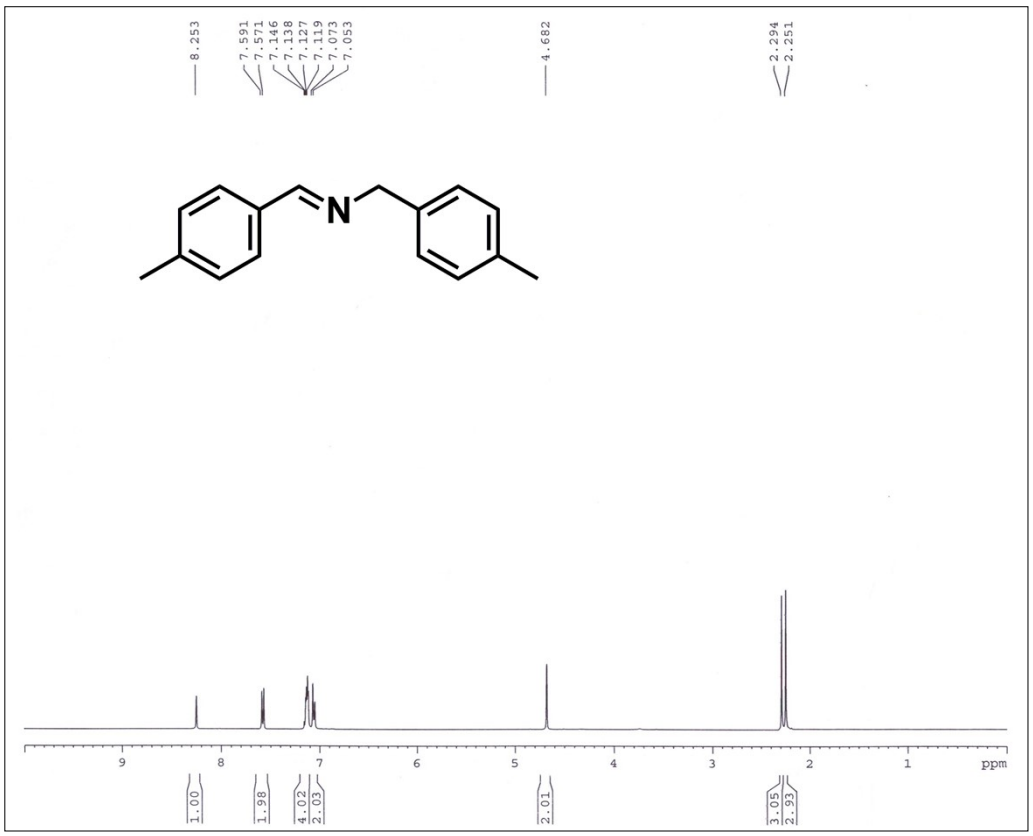

Figure S25. [1]H NMR data of N-(4-methylbenzyl)1-(*p*-tolyl) methanimine.

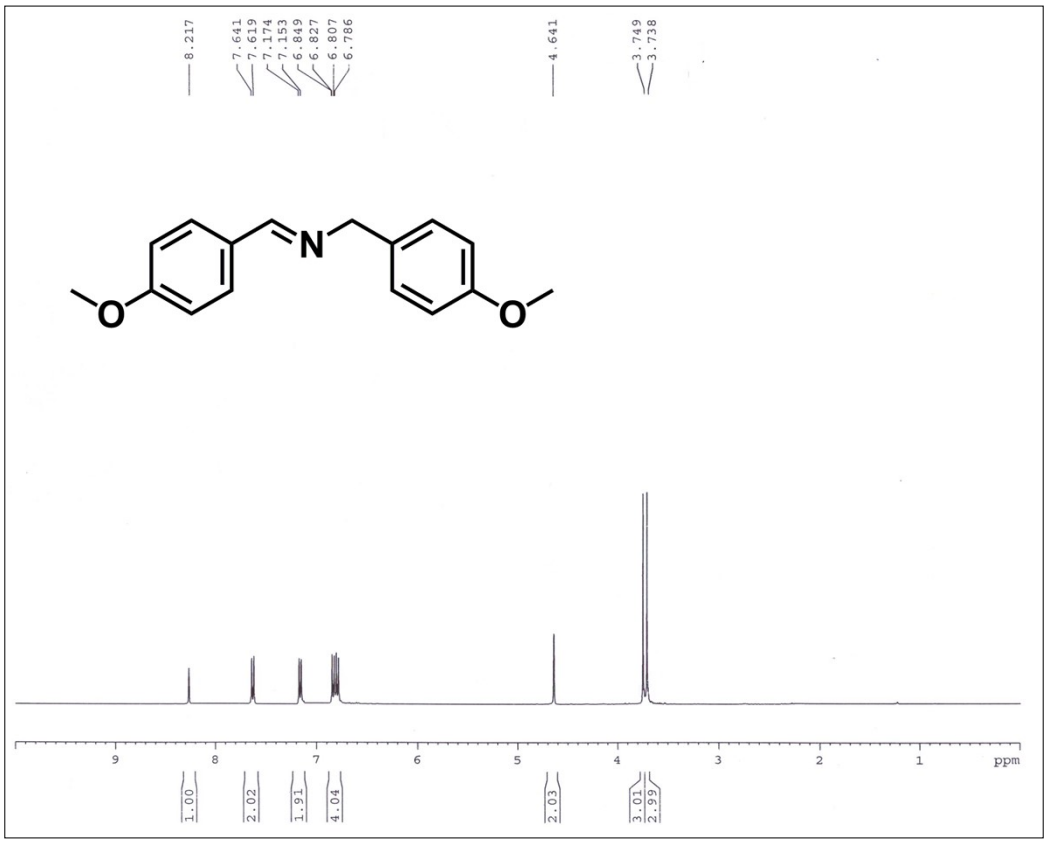

Figure S26. [1]H NMR data of N-(4-methoxybenzyl)-1-(4-methoxyphenyl) methanimine.

Figure S27. [1]H NMR data of N-(4-fluorobenzyl)-1-(4-fluorophenyl) methanimine.

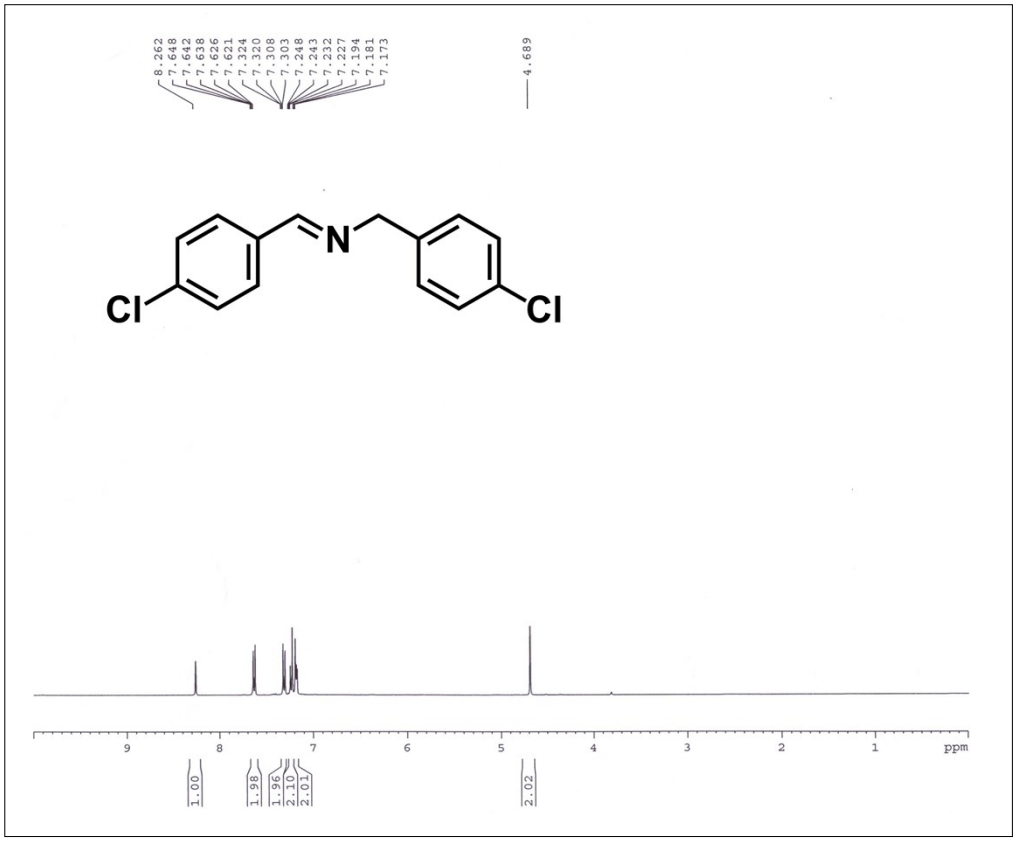

Figure S28. [1]H NMR data of N-(4-chlorobenzyl)-1-(4-chlorophenyl) methanimine.

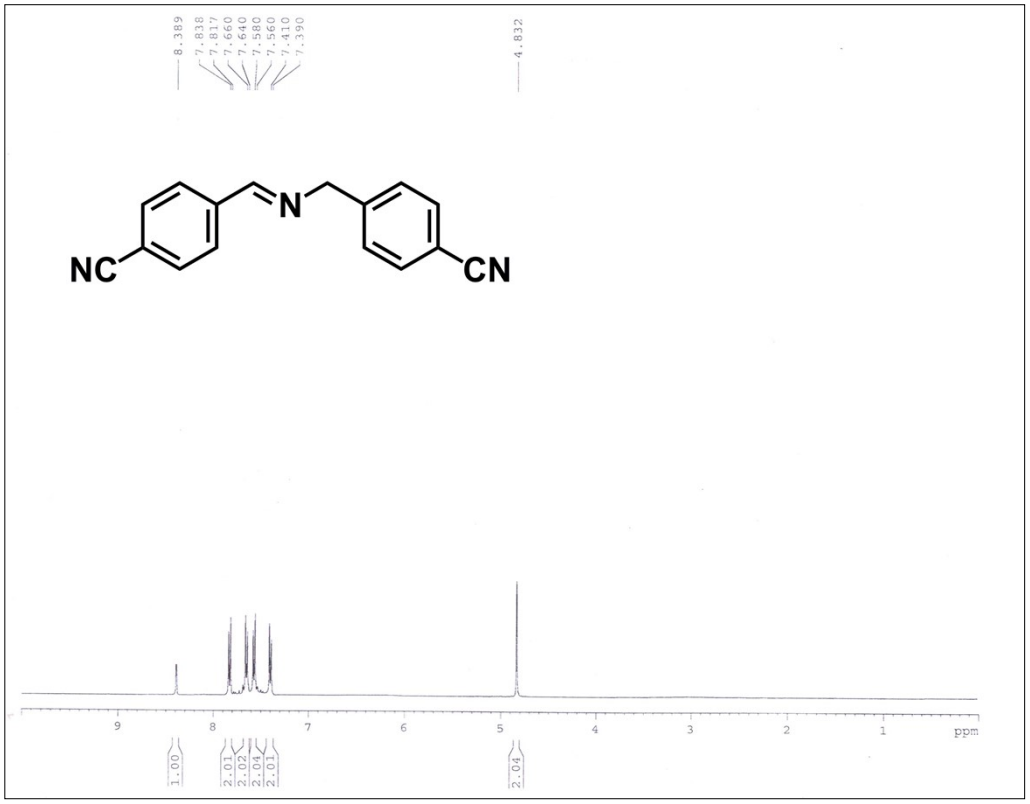

Figure S29. [1]H NMR data of 4-(((4-cyanobenzyl) imino) methyl) benzonitrile.

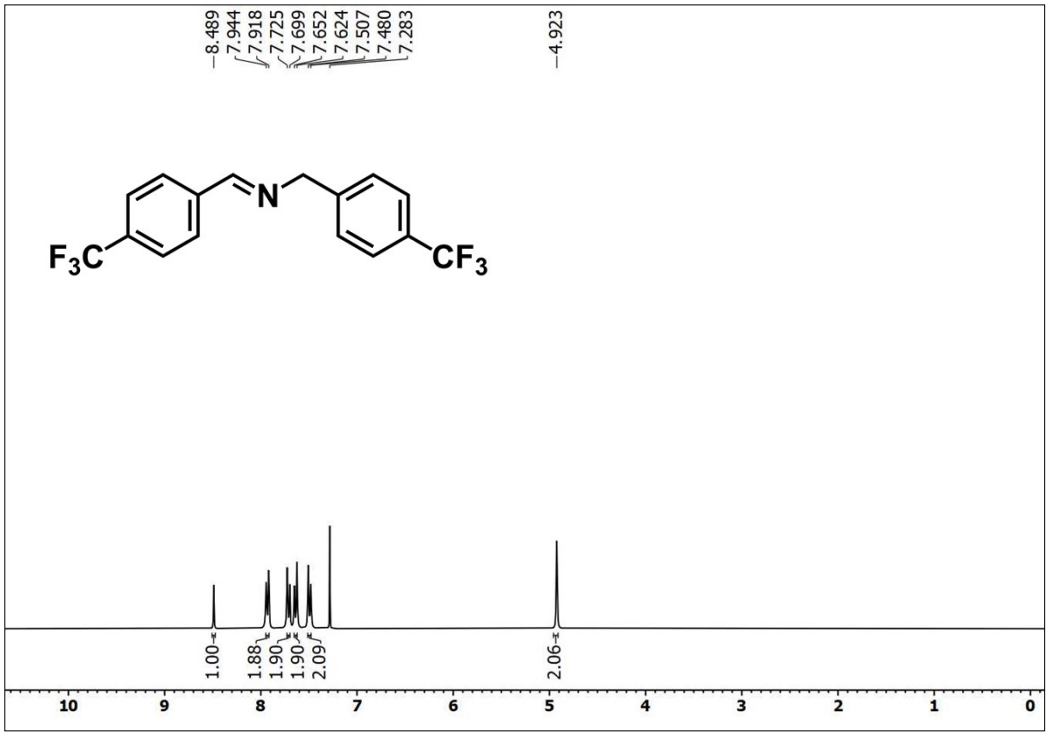

Figure S30. ^{1}H NMR data of N-(4-(trifluoromethyl) benzyl)-1-(4-fluoromethyl) phenyl) methanimine.

Figure S31. ^{1}H NMR data of N-(3-methoxybenzyl)-1-(3-methoxyphenyl) methanimine.

Figure S32. [1]H NMR data of N-(3-bromobenzyl)-1-(3-bromophenyl) methanimine.

Figure S33. [1]H NMR data of N,1-diphenylmethanimine.

^{1}H NMR data of N-benzylidene benzylamine amine and benzaldehyde derivatives in presence of O_2:

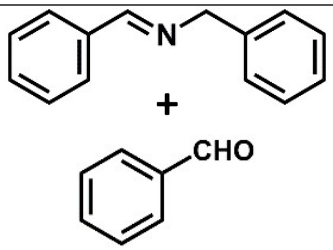	N-benzylidene benzylamine, ^{1}H NMR (400 MHz, $CDCl_3$), δ (ppm): 8.433 (s, 1H), 7.836-7.801 (m, 2H), 7.460-7.426 (m, 3H), 7.376-7.365 (d, *J*=4.4 Hz, 4H), 7.310-7.266 (m, 1H), 4.858 (s, 2H). Benzaldehyde, ^{1}H NMR (400 MHz, $CDCl_3$), δ (ppm): 10.052 (s, 1H), 7.922-7.900 (m, 2H), 7.590-7.542 (m, 3H).
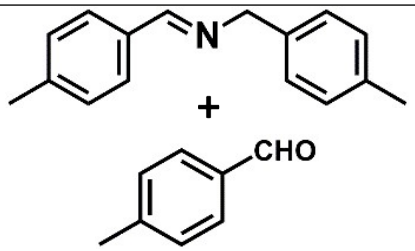	N-(4-methylbenzyl)1-(*p*-tolyl) methanimine, ^{1}H NMR (400 MHz, $CDCl_3$), δ (ppm): 8.298 (s, 1H), 7.631-7.611 (d, *J*=8.0 Hz, 2H), 7.202-7.158 (m, 4H), 7.113-7.093 (d, *J*=8.0 Hz, 2H), 4.727 (s, 2H), 2.339 (s, 3H), 2.296 (s, 3H). 4-methylbenzaldehyde, ^{1}H NMR (400 MHz, $CDCl_3$), δ (ppm): 9.876 (s, 1H), 7.742-7.722 (d, *J*=8.0 Hz, 2H), 7.294-7.274 (d, *J*=8.0 Hz, 2H), 2.399 (s, 3H).
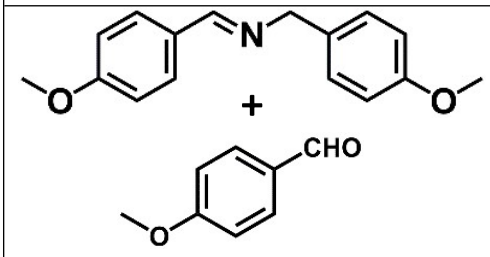	N-(4-methoxybenzyl)-1-(4-methoxyphenyl) methanimine, ^{1}H NMR (400 MHz, $CDCl_3$), δ (ppm): 8.226 (s, 1 H), 7.681–7.659 (d, *J*=8.4 Hz, 2H), 7.214-7.193 (d, *J*=8.4 Hz, 2H), 6.889-6.826 (m, 2H), 4.643 (s, 2H), 3.751 (s, 3H), 3.711 (s, 3H). 4-methoxybenzaldehyde, ^{1}H NMR (400 MHz, $CDCl_3$), δ (ppm): 9.80 (s, 1H), 7.808-7.786 (dd, *J*=8.8, 2.0 Hz, 2H), 6.971-6.949 (d, *J*=8.8 Hz, 2H), 3.802 (s, 3H).

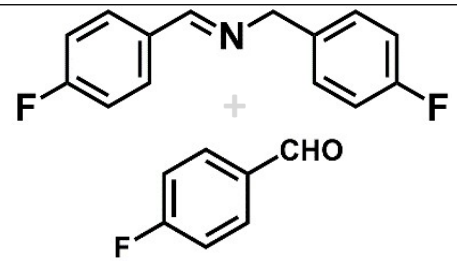	N-(4-fluorobenzyl)-1-(4-fluorophenyl)methanimine, ^{1}H NMR (400 MHz, $CDCl_3$), δ (ppm): 8.306 (s, 1 H), 7.747–7.711 (m, 2H), 7.271-7.236 (m, 2H), 7.083-6.969 (m, 4H), 4.721 (s, 2H). 4-fluorobenzaldehyde, ^{1}H NMR (400 MHz, $CDCl_3$), δ (ppm): 9.925 (s, 1H), 7.887-7.851 (m, 2H), 7.196-7.175 (d, *J*=8.4 Hz, 2H).
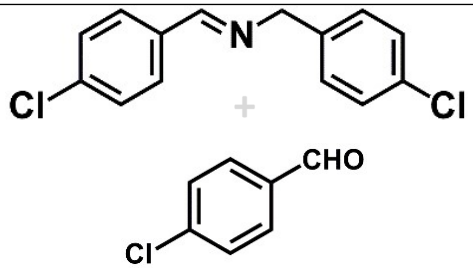	N-(4-chlorobenzyl)-1-(4-chlorophenyl)methanimine, ^{1}H NMR (400 MHz, $CDCl_3$), δ (ppm): 8.322 (s, 1 H), 7.710–7.676 (m, 2H), 7.386-7.365 (m, 2H), 7.315-7.234 (m, 4H), 4.748 (s, 2H). 4-chlorobenzaldehyde, ^{1}H NMR (400 MHz, $CDCl_3$), δ (ppm): 9.963 (s, 1H), 7.817-7.796 (m, 2H), 7.489-7.482 (d, *J*=2.8 Hz, 2H).
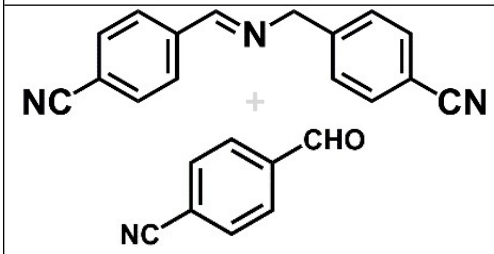	4-(((4-cyanobenzyl)imino)methyl)benzonitrile, ^{1}H NMR (400 MHz, $CDCl_3$) δ (ppm): 8.383 (s, 1H), 7.836-7.816 (d, *J*=8 Hz, 2H), 7.659-7.639 (d, *J*=8.0 Hz, 2H), 7.577-7.557 (d, *J*=8.0 Hz, 2H), 7.387-7.366 (d, *J*=8.4 Hz, 2H), 4.813 (s, 2H). 4-formylbenzonitrile, ^{1}H NMR (400 MHz, CDCl3), δ (ppm): 10.023 (s, 1H), 8.056-8.035 (d, *J*=8.4 Hz, 2H), 7.936-7.915 (d, J=8.4 Hz, 2H).

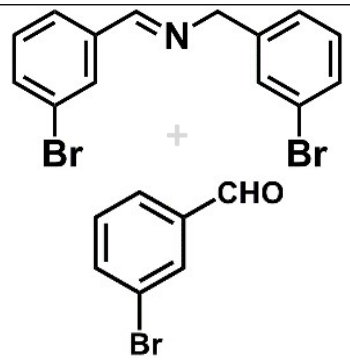	N-(3-bromobenzyl)-1-(3-bromophenyl)methanimine, ^{1}H NMR (400 MHz, $CDCl_3$), δ (ppm): 8.225 (s, 1 H), 7.880–7.871 (t, *J*= 3.6 Hz, 1H), 7.590-7.564 (m, 1H), 7.479-7.456 (m, 1H), 7.325-7.297 (m, 1H), 7.216-7.099 (m, 4H), 4.683 (s, 2H). 3-bromobenzaldehyde, ^{1}H NMR (400 MHz, $CDCl_3$), δ (ppm): 9.878 (s, 1H), 7.961 (s, 1H), 7.724-7.705 (d, *J*=7.6 Hz, 2H), 7.533-7.528 (t, 1H).
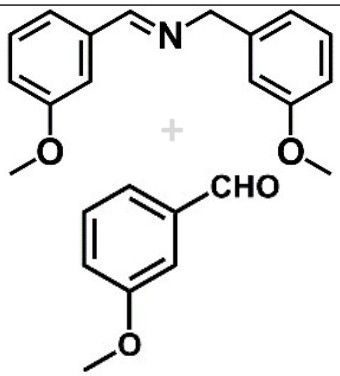	N-(3-methoxybenzyl)-1-(3-methoxyphenyl)methanimine, ^{1}H NMR (400 MHz, $CDCl_3$) δ (ppm): 8.373 (s, 1H), 7.309 (s, 1H), 7.242-7.145 (m, 3H), 6.921-6.874 (m, 1H), 6.845-6.812 (m, 2H), 6.732-6.704 (dd, *J*=8.4, 2.8 Hz, 1H), 4.685 (s, 2H), 3.717 (s, 3H), 3.685 (s, 3H). 3-methoxybenzaldehyde, ^{1}H NMR (400 MHz, $CDCl_3$), δ (ppm): 9.990 (s, 1H), 7.356-7.328 (m, 2H), 7.287-7.285 (m, 1H), 7.095-7.059 (m, 1H), 3.735 (s, 3H).

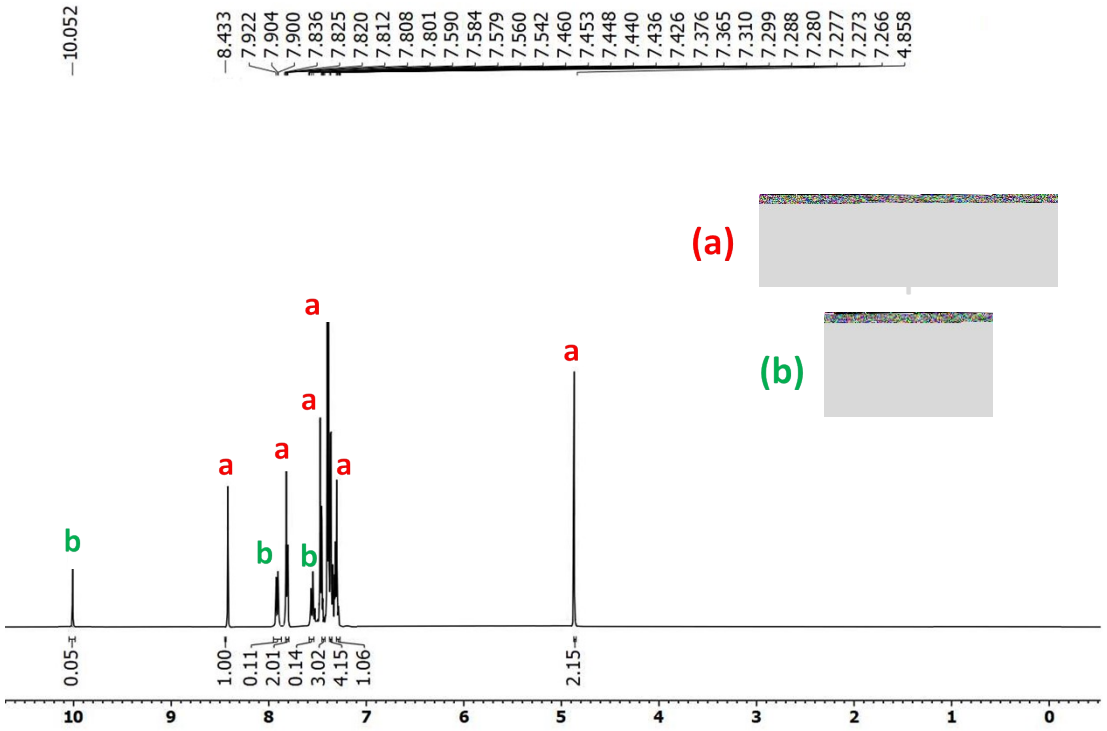

Figure S34. [1]H NMR data of N-benzylidene benzylamine and benzaldehyde

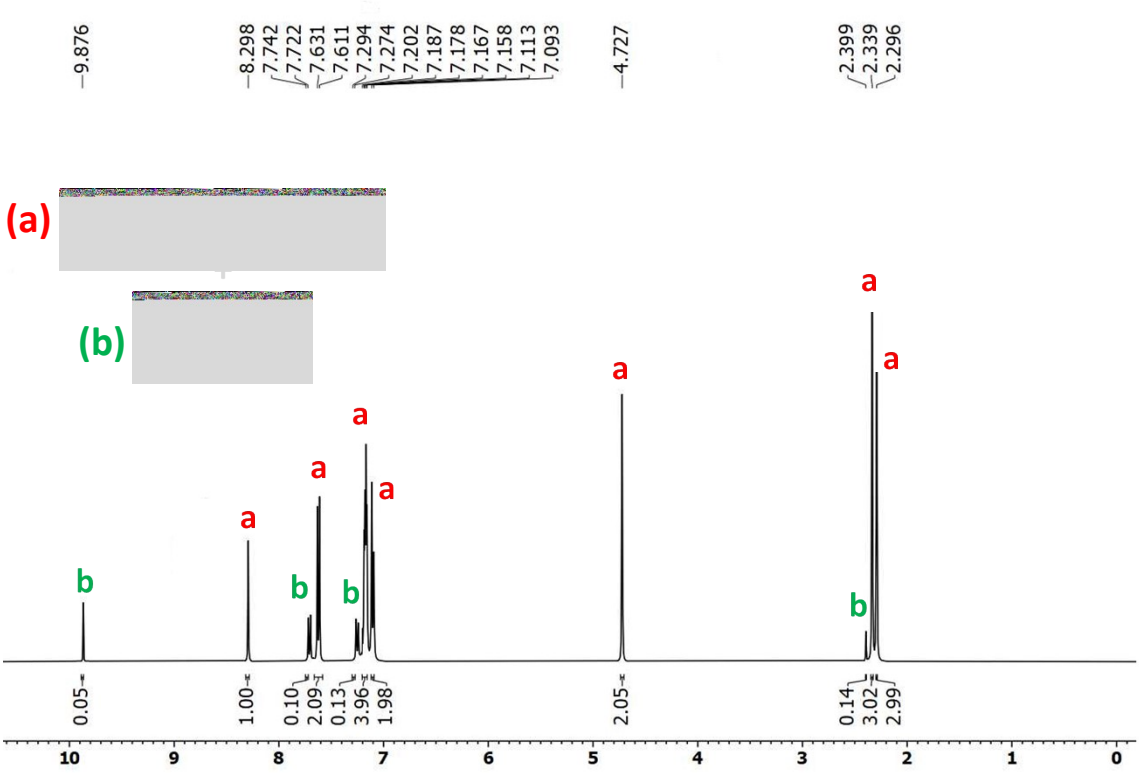

Figure S35. [1]H NMR data of N-(4-methylbenzyl)1-(*p*-tolyl) methanimine and 4-Methylbenzaldehyde

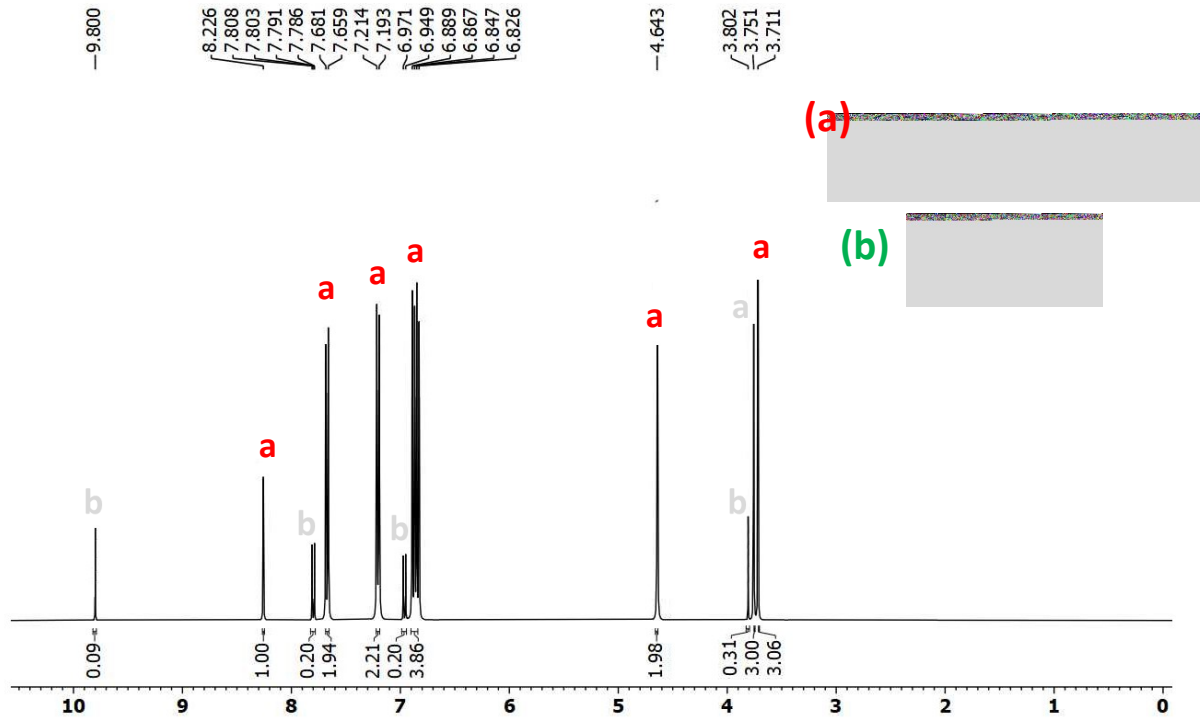

Figure S36. [1]H NMR data of N-(4-methoxybenzyl)-1-(4-methoxyphenyl)methanimine and 4-Methoxybenzaldehyde

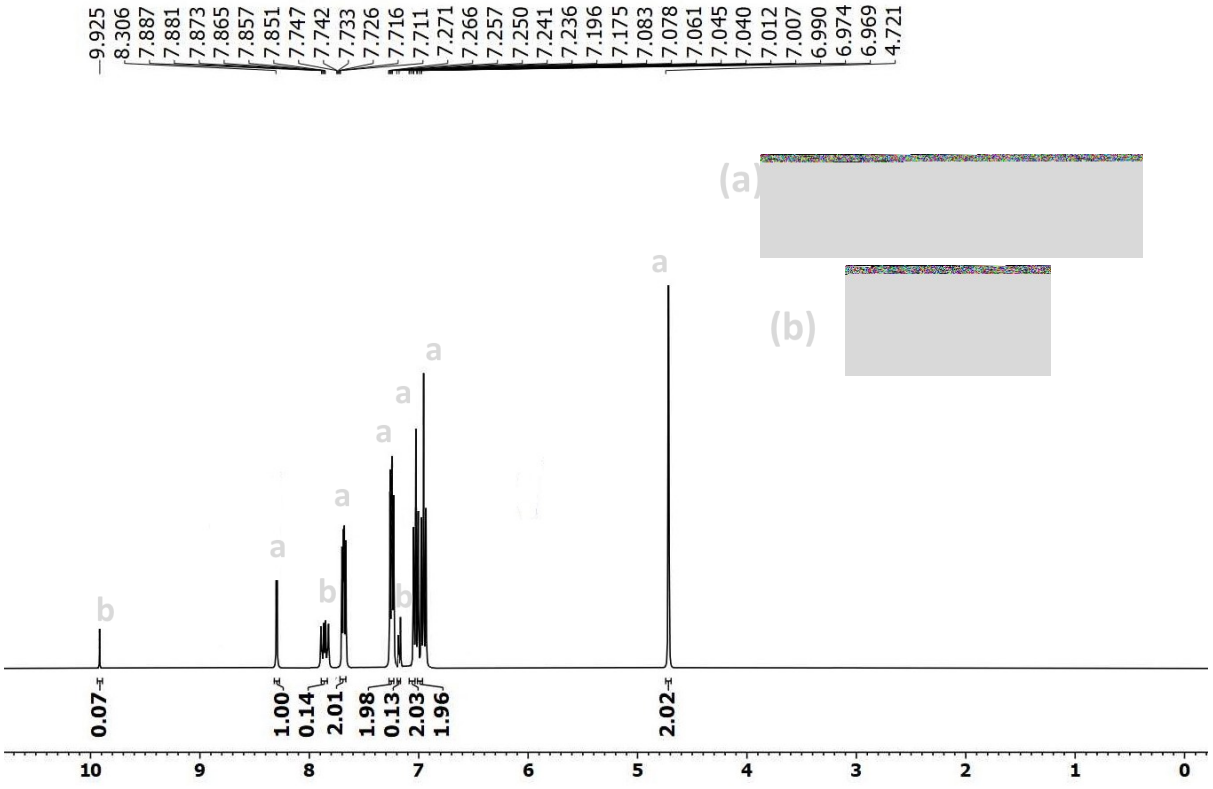

Figure S37. [1]H NMR data of N-(4-fluorobenzyl)-1-(4-fluorophenyl)methanimine and 4-fluorobenzaldehyde

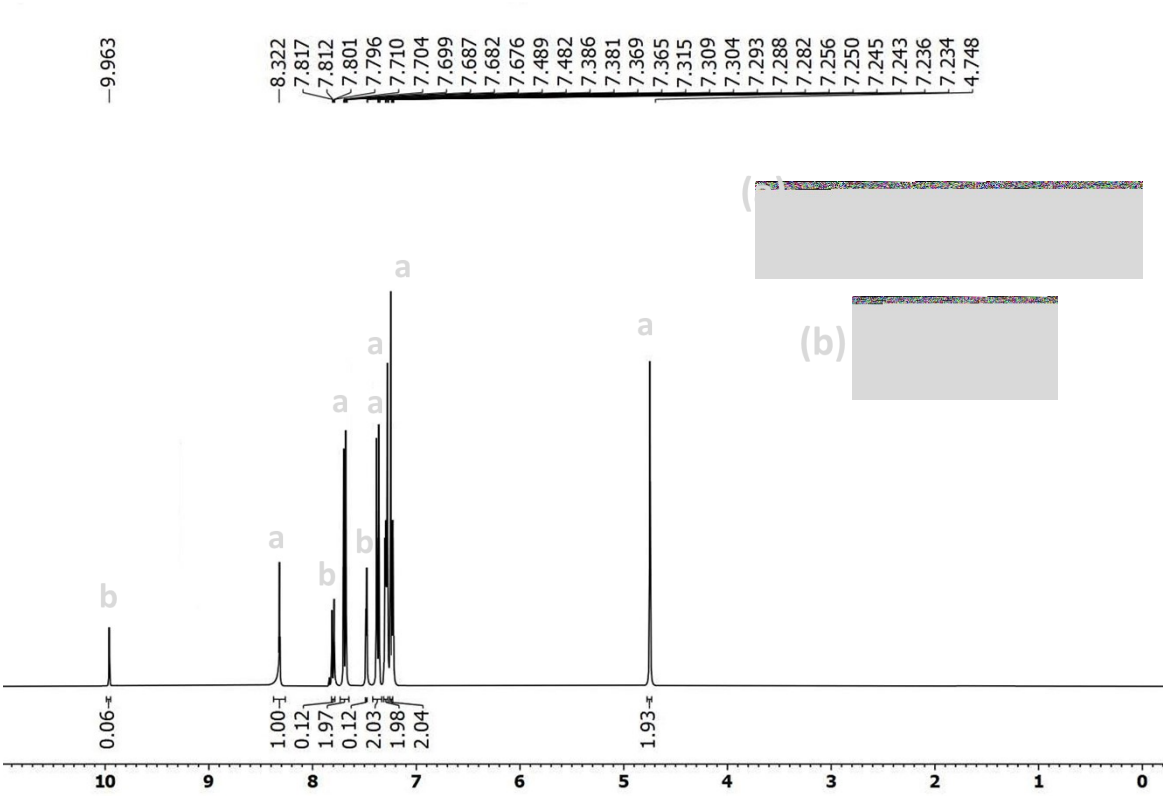

Figure S38. [1]H NMR data of N-(4-chlorobenzyl)-1-(4-chlorophenyl)methanimine and 4-Chlorobenzaldehyde

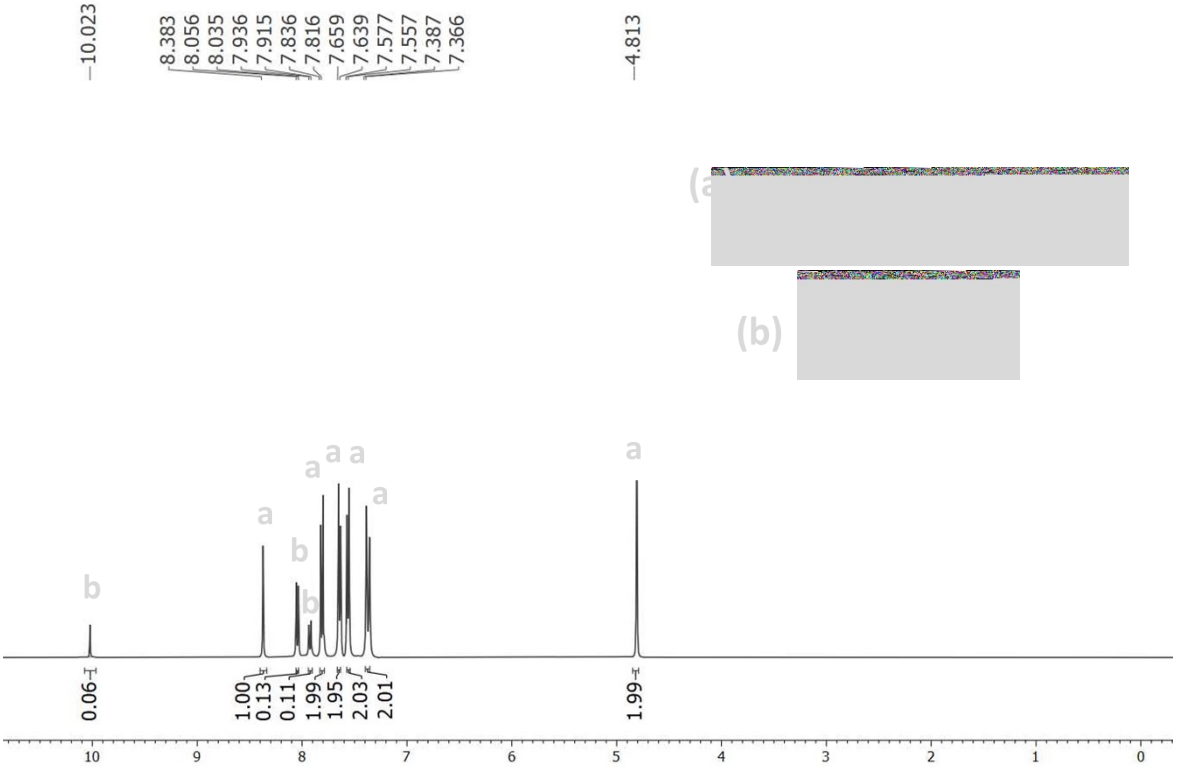

Figure S39. [1]H NMR data of 4-(((4-cyanobenzyl)imino)methyl)benzonitrile and 4-formylbenzonitrile

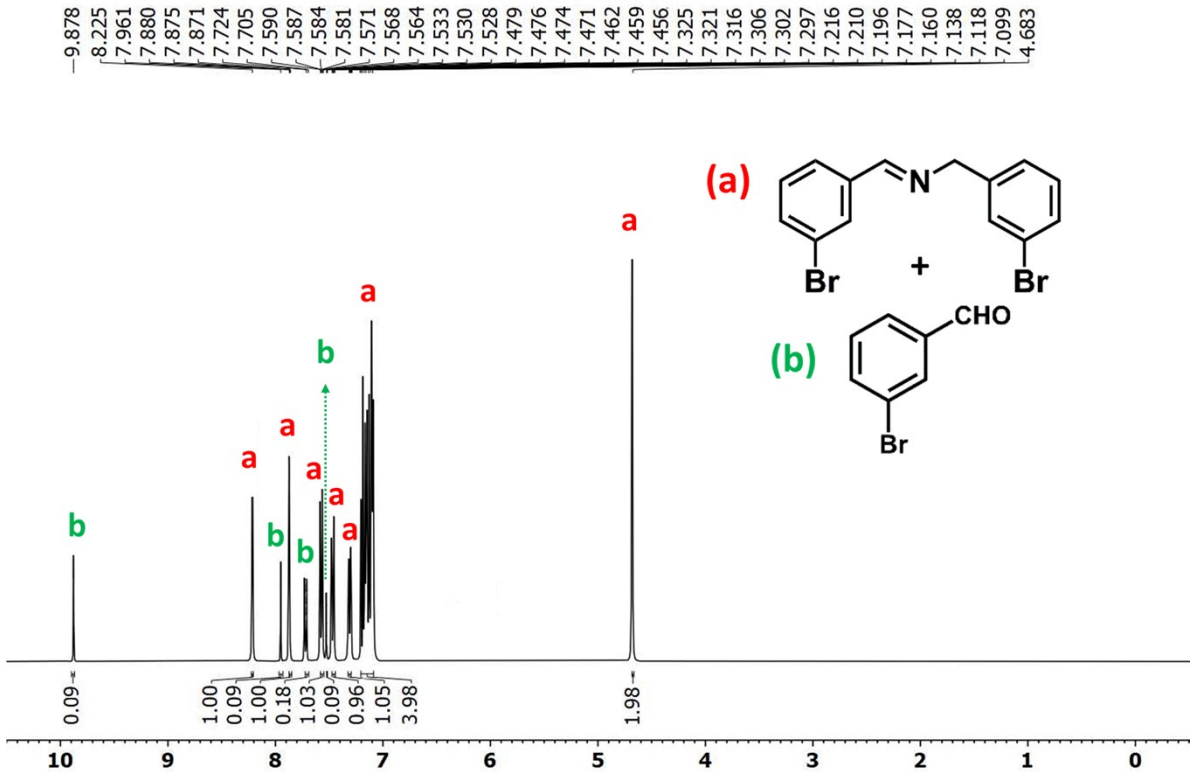

Figure S40. [1]H NMR data of N-(3-bromobenzyl)-1-(3-bromophenyl) methanimine and 3-bromobenzaldehyde

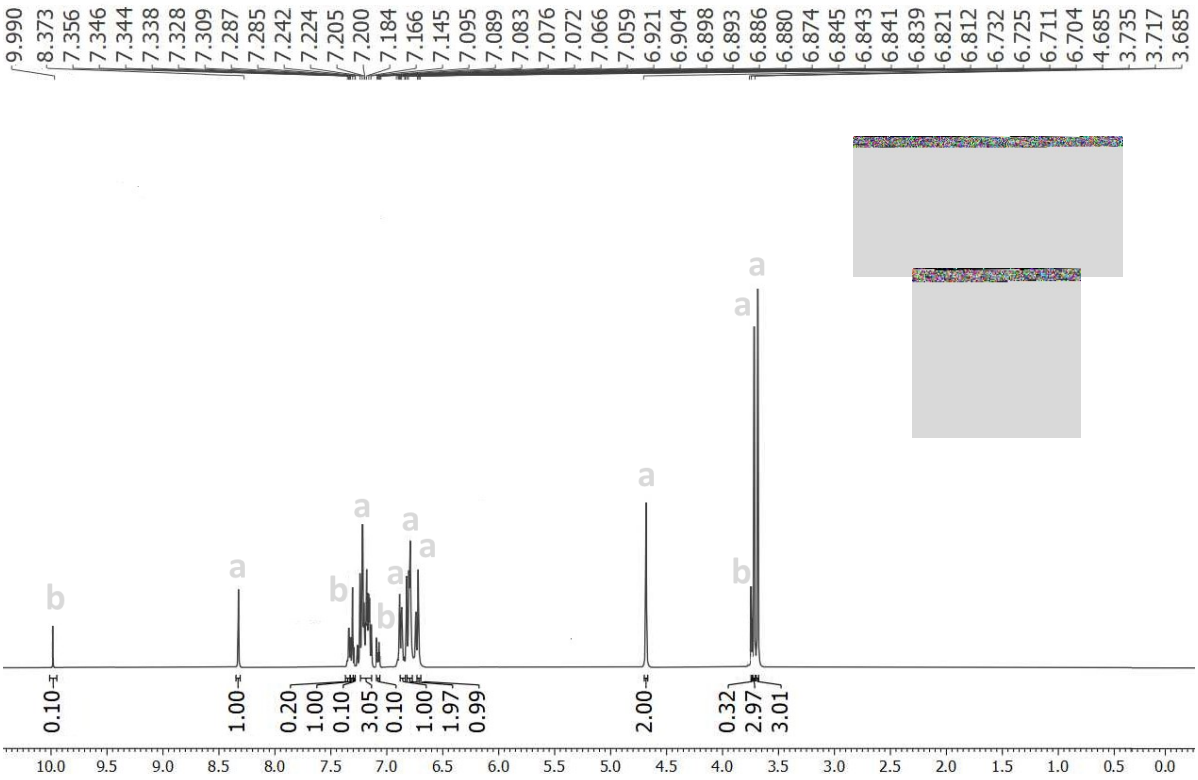

Figure S41. [1]H NMR data of N-(3-methoxybenzyl)-1-(3-methoxyphenyl)methanimine and 3-methoxybenzaldehyde.

Reference

1. J. H. Chong, M. Sauer, B. O. Patrick and M. J. MacLachlan, *Org. Lett*., 2003, **21**, 3823-3826.
2. Y. Li, W. Chen, R. Gao, Z. Zhao, T. Zhang, G. Xing and L. Chen, *Chem. Commun.*, 2019, **55**, 14538-14541.